NASA Technical Memorandum 85963

Airborne Astronomy Program
Medium Altitude Missions Branch
Preprint Series 018

NASA-TM-85963 19840018458

The Nature of AFGL 2591 and its Associated Molecular Outflow: Infrared and Millimeter-Wave Observations

Charles J. Lada,
Harley A. Thronson, Jr.,
Howard A. Smith, P.R. Schwartz,
and W. Glaccum

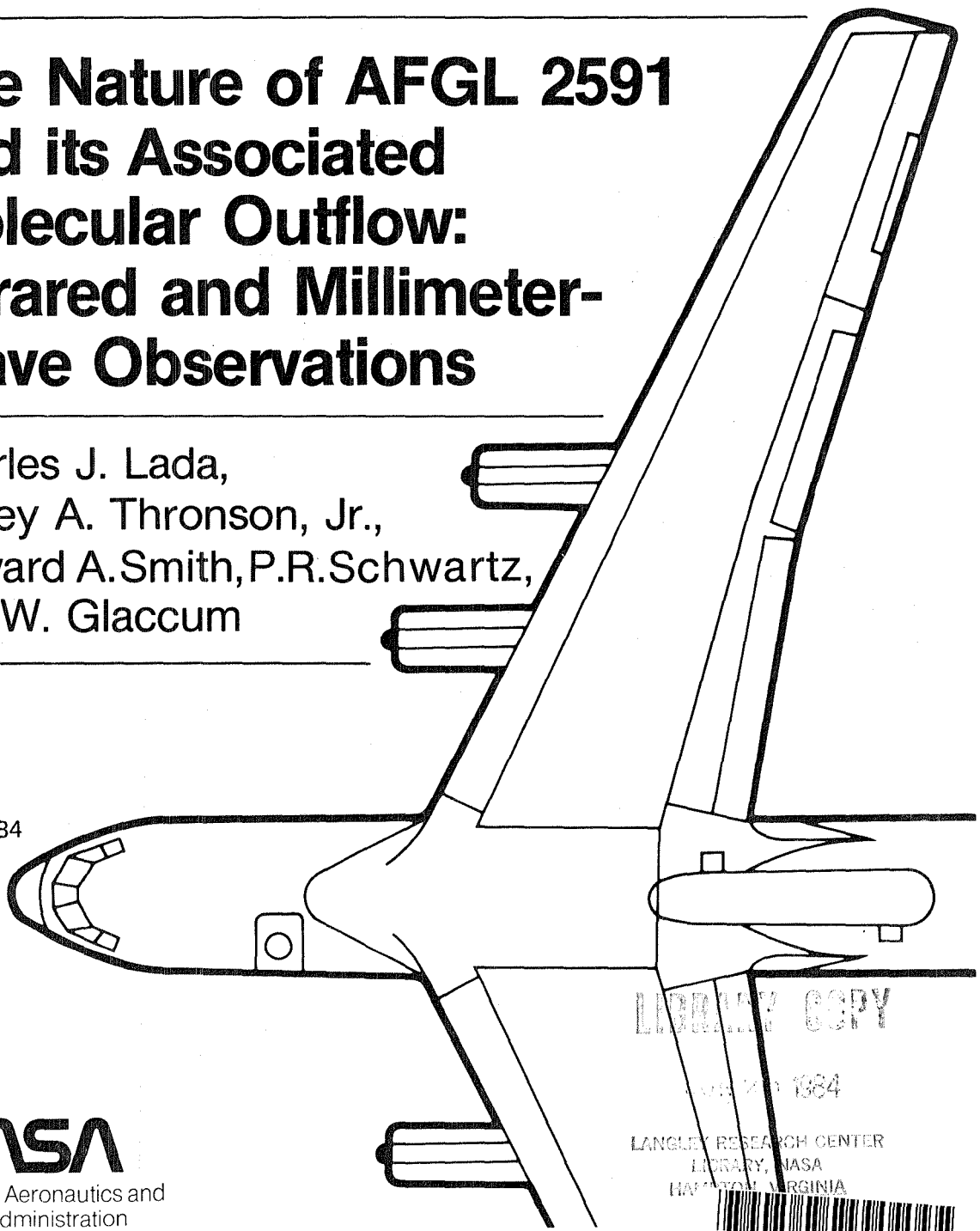

May 1984

National Aeronautics and
Space Administration

NASA Technical Memorandum 85963

Airborne Astronomy Program
Medium Altitude Missions Branch
Preprint Series 018

The Nature of AFGL 2591 and its Associated Molecular Outflow: Infrared and Millimeter-Wave Observations

Charles J. Lada, Steward Observatory, University of Arizona and
Wyoming Infrared Observatory, University of Wyoming

Harley A. Thronson, Jr., Wyoming Infrared Observatory, University of Wyoming

Howard A. Smith
P. R. Schwartz, E. O. Hulburt Center for Space Research, Naval Research Lab

W. Glaccum, Yerkes Observatory, University of Chicago

National Aeronautics and
Space Administration

Ames Research Center
Moffett Field, California 94035

THE NATURE OF AFGL 2591 AND ITS ASSOCIATED MOLECULAR OUTFLOW: INFRARED AND MILLIMETER-WAVE OBSERVATIONS

Charles J. Lada[1]
Steward Observatory
University of Arizona
and
Wyoming Infrared Observatory
University of Wyoming

Harley A. Thronson, Jr.
Wyoming Infrared Observatory
University of Wyoming

Howard A. Smith and P. R. Schwartz
E. O. Hulburt Center for Space Research
Naval Research Lab

W. Glaccum
Yerkes Observatory
University of Chicago

Received: 1983 October 19

[1] Alfred P. Sloan Foundation Fellow

ABSTRACT

The results of infrared photometry from 2 μm-160 μm of AFGL 2591 and ^{12}CO observations of its associated molecular cloud and high velocity molecular outflow are presented and discussed. Observations between 60 μm and 160 μm provide the first detailed far-infrared spectrum of this source. The observed luminosity between 2 and 160 μm is 6.7×10^4 $L_\odot$ at a distance of 2 kpc. We estimate the total luminosity to be $\sim 9 \times 10^4$ $L_\odot$. The 2 μm to 160 μm spectrum of AFGL 2591 is interpreted in the context of a model in which a single embedded object is the dominant source of the infrared luminosity. We determine this object to be surrounded by a compact, optically thick dust shell with a temperature in excess of several hundred degrees kelvin. We estimate the extinction to this source to be between 26 and 50 visual magnitudes. Our data is consistent with earlier suggestions that the object which powers the near-infrared source also is responsible for ionizing the compact HII regions near AFGL 2591. We have determined the absolute position of the infrared source at 10 μm to an accuracy of ± 1". This indicates for the first time that the IR source and H_2O source are not coincident.

Our ^{12}CO observations show the high-velocity molecular flow near AFGL 2591 to be extended, bipolar and roughly centered on the infrared emission. The observations suggest that the red-shifted flow component extends beyond the boundary of the ambient cloud within which AFGL 2591 is embedded. The ^{12}CO observations also show that AFGL 2591 is embedded in a molecular cloud with an LSR velocity of -5 km s^{-1}. Comparing this velocity with the velocity of H_2O maser emission ($\sim$ -22 km s^{-1}) suggests

that the maser source is part of the blue-shifted high-velocity molecular outflow. Its close proximity to the infrared source suggests that the origin of the molecular outflow may be very close to (within 1") the surface of AFGL 2591.

I. INTRODUCTION

The observation that most stars, in their earliest stages of stellar evolution, produce cold energetic outflows of molecular gas (e.g., Bally and Lada 1983) suggests a revision of our understanding of the nature of young embedded infrared sources (e.g., Wynn-Williams 1982). It is now clear that many objects previously thought to be quietly accreting protostars are actually the centers of very energetic mass explusion. One such object, AFGL 2591, typical of the proto-stellar sources, has recently been found to be associated with a high-velocity molecular outflow (Bally and Lada 1983, Torrelles et al 1983). AFGL 2591 is a very compact ($\lesssim$ 0.2", Howell, McCarthy and Low 1981) and luminous ($L \gtrsim 3 \times 10^4 L_\odot$, Merill and Soifer 1974) near-infrared source. It is closely associated with an H_2O maser source (Wynn-Williams 1977) and also near at least two, weak compact HII regions (e.g. Simon et al 1981). Although very luminous and compact, there is no evidence for ionized emission at the location of the near-infrared source (Thompson and Tokunaga 1979, Simon et al 1981), suggesting that the source has not yet evolved to the stage of emitting significant ionizing flux. Despite extensive near-infrared studies, little is known about the far-infrared spectrum of this object and its total luminosity has not been accurately determined. The recent detection of high-velocity molecular flow around this object and the lack of a good far-infrared spectrum of this object motivated us to obtain further observations of this source and reconsider its nature. In particular we were interested in determining the characteristics of

the molecular flow and its relation to the infrared source, compact HII regions and water maser. We also were interested in obtaining a good far-infrared spectrum in order to obtain a reliable total luminosity and investigate the detailed energetics of the source.

To accomplish these objectives we obtained new millimeter-wave CO and infrared observations of AFGL 2591. The results of these observations, which include the detection of a bipolar molecular flow and the first accurate far-infrared spectrum of this source, are presented in this paper. We also present new 2-20 μm broadband spectroscopy of the near-infrared source and a 10 μm absolute position measurement of the source, which significantly improves upon previous determinations made at shorter wavelengths. The telescopes and observing techniques employed for this study are described in Section II, the results and analysis of observations in Section III and the implications of the results in Section IV and Section V.

II. TELESCOPES AND OBSERVING TECHNIQUES

a) Millimeter-wave Spectroscopy

Observations of the J=1-0 transition of $^{12}C^{16}O$ at 2.6 mm were initially obtained in 1981 February with the 11-meter millimeter-wave telescope of the National Radio Astronomy Observatory (NRAO)[2] in Arizona. Subsequently the majority of the observations reported here were obtained in 1983 June with the new 12-meter surface of the NRAO millimeter-wave telescope. Both sets of CO observations were made with the same cooled, dual-channel, mixer receiver which was operated in conjunction with a 512-channel filter bank spectrometer, which provided spectral resolutions of 0.25 MHz and 0.50 MHz. The filters were split so that each polarization channel of the receiver was coupled to two independent 128-channel banks of 0.50 MHz and 0.25 MHz filters respectively. Data taken at the same resolution in the two receiver channels were averaged together. All spectra were observed in the position switching mode using the same "off" position (i.e. $\alpha = 20^h2\ ^m35^s.9$, $\delta = 43°\ 01'16"$; 1950.0) which was pre-determined to be free of significant ^{12}CO emission. Data taken with both telescopes were initially calibrated using a rotating chopper wheel following Ulich and Haas (1976). The 11-m data were finally calibrated by observing Orion

---

[2]The National Radio Astronomy Observatory is operated by the Associated Universities, Inc., under contract with the National Science Foundation.

and IRC +10° 216 and adopting temperature scales such that T_A^* = 60.0 K and T_A^* = 4.1 K for these two objects respectively. Final calibrations for the 12-m data was accomplished by observing M17 SW and IRC +10° 216 and adopting the observed temperatures T_A^* = 35.2 K and T_A^* = 5.8 K for these two objects respectively. The M17SW temperature agrees within 10% with standard 11-m value of T_A^* = 39.0 K (Thronson and Lada 1983, Ulich and Haas 1976) while the value for IRC +10° 216 is 38% higher than the standard 11-m calibration. This is an expected result of the higher aperture efficiency of the 12-m surface.

b) Near- and Mid-Infrared Photometry

AFGL 2591 was observed during the autumn of 1982 using a Ge(Ga) bolometer system on the 2.3 m telescope of the Wyoming Infrared Observatory (WIRO). Observations were obtained with broadband filters centered at the wavelengths listed in Table 2 and used a 6.6" aperture and a chopping secondary with a 30" north-south throw. The filter characteristics and absolute calibrations are the same as presented by Gehrz, Hackwell and Jones (1974). The internal uncertainty for these observations was less than 2% in flux (1σ RMS). Therefore, the total uncertainty is dominated by systematic errors in the absolute calibration of standard sources. We estimate this uncertainty to be ±5% at 2.3 μm, 3.6 μm and 4.9 μm, and ±10% at the longer wavelengths.

c) Far-Infrared Photometry

AFGL 2591 was observed during 1982 August at far-infrared wavelengths using the 0.9 m telescope onboard NASA's Kuiper Airborne Observatory (KAO). A multi-channel, multi-filter Ge(Ga) system was used to map the source over an area of 3' x 6' (east-west by north-south). The angular resolution of the system was 49". Four filters with effective center wavelengths of 60 μm, 95 μm, 110 μm, and 160 μm were used to obtain far-infrared flux densities. The absolute calibration uncertainty in the flux density is approximately ±20%. The statistical uncertainty was about ±1% (1σ RMS) and therefore can be ignored. Details concerning filter characteristics and calibration procedures have been described elsewhere (Thronson and Harper 1979, Loewenstein et al. 1977). The W3(OH) source was used for calibration. Data were taken by chopping the secondary to a reference position 7.5' north and south of AFGL 2591. The maximum far-infrared emission was located at the 10 μm peak, within the ±15" positional uncertainty, and the object was unresolved. Weak, extended emission was observed from the source throughout the region mapped, but at a level 0.5-1% of the peak channel. It is unlikely that this flux contributes more than ∿ 20% to the total measured at the peak of AFGL 2591.

III. RESULTS AND ANALYSIS

a) CO Observations

Spectra of $^{12}C^{16}O$ emission were obtained at 21 locations in a grid centered on AFGL 2591. Ten positions were observed with the 11-m telescope and 14 positions with the 12-m telescope, while three positions were observed in common with both telescopes. At the infrared peak of AFGL 2591, the spectrum consists of two strong but narrow emission line components superposed upon broad emission wings which extend over about 40 km s^{-1} (e.g. Bally and Lada 1983, Torrelles et al 1983). The strongest narrow line component is at a velocity of about -5 km s^{-1}, and the weaker component at about +1 km s^{-1}. The temperatures of the two components centered on AFGL 2591 are T_A^* = 15.2 K (-5 km s^{-1}) and T_A^* = 5.1 K (+1 km s^{-1}) when observed with the 11 m telescope and T_A^* = 18.5 K (-5 km s^{-1}) and T_A^* = 5.4 K (+1 km s^{-1}) when observed with the 12 m telescope. The difference in the two sets of observations is apparently a result of the fact the +1 km s^{-1} component is considerably more extended than the -5 km s^{-1} component. The higher aperture efficiency of the 12 m surface will result in a larger antenna temperature for less extended objects. In fact, at the positions observed in common the antenna temperatures of the +1 km s^{-1} component agree to within 10% while the -5 km s^{-1} component is systematically stronger by about 20% in two positions (0,0 and 1W,1S). This suggest that emission from -5 km s^{-1} does not fill the beam uniformly and is clumpy. To make a map of the distribution of emission of the -5 km s^{-1}

component, we scaled the 12-m data to match the 11-m data at the position of AFGL 2591. The results are shown in Figure 1 in the form of a contour map of $T_A^*(-5 \text{ km s}^{-1})$. The positions where spectra were observed are also indicated on the map by crosses. We find that the ^{12}CO emission (at -5 km s^{-1}) peaks on AFGL 2591, which is also apparent when both sets of data are treated separately. The clear intensity enhancement of the -5 km s^{-1} cloud at the position of AFGL 2591 suggests that the infrared source is embedded in this cloud. Emission at -5 km s^{-1} falls off rapidly to the northeast of AFGL 2591, but more gradually to the southwest. On the other hand, there appears to be little variation in the intensity of the 1 km s^{-1} component across the mapped grid. This can be seen in Table 1 where we list the observed antenna temperatures of the 1 km s^{-1} component at each position of the grid. At most locations the antenna temperature of this component is within 0.5 K of $T_A^* = 5.0$ K. This confirms our earlier suggestion that the 1 km s^{-1} cloud is extended and uniform.

In order to investigate the distribution of high-velocity CO emission around AFGL 2591, we determined the integrated intensities in the red and blue high-velocity wings for CO profiles at each position in the grid as follows:

$$\text{RED} = \int_{3.8}^{14.5} T_A^* dv \qquad \text{and} \qquad \text{BLUE} = \int_{-21.9}^{-10.2} T_A^* dv$$

These integrated intensities are also listed in Table 1. The maximum values occur near AFGL 2591 and in the blue component, which at the infrared source is four times stronger than the red component. However, there is considerable variation of the ratio of BLUE/RED across the source and our observations clearly show the flow in AFGL 2591 to be bipolar. The approximate boundaries of the regions where the integrated intensities in the red and blue components exceed 3 K-km s^{-1} are indicated in Figure 1. Again the bipolar nature of this flow is apparent. Figure 2 shows spectra obtained at two positions in the flow marked with x's in Figure 1. They dramatically illustrate the distinct spatial separation of the red and blue high-velocity flow components. Indeed, the most intense high-velocity emission we measured in the red flow occurs at the edge of our grid, apparently well beyond the boundary of the -5 km s^{-1} cloud. Unfortunately we did not observe enough positions to determine the true extent and distribution of the high-velocity gas. In addition, we did not obtain ^{13}CO observations and we are unable to reliably estimate either the masses or the energetics for the high-velocity flow. Recent observations by Torrelles et al (1983) of a similar sized region around AFGL 2591 with the 11-m telescope did not indicate a bipolar nature to the high-velocity emission. However, their data did not have sufficient signal-to-noise to detect the red component of the flow and were only sensitive enough to map the distribution of the brightest high-velocity blue-shifted gas. Their map of the blue component of the high-velocity flow is in satisfactory agreement with our results.

b) Infrared Observations

The results of our infrared photometry from 2 to 160 μm are presented in Table 2. The resulting spectrum is plotted in Figure 3. Our 2-20 μm spectrum agrees well with previously published observations (Merrill and Soifer 1974; Willner et al 1982). The spectrum is very similar to "protostars" such as BN, W3 IRS 5 and NGC 7538 IRS 9, objects all associated with high-velocity molecular flows. Integrating under the observed spectrum we obtain the first accurate luminosity for this source. We find $L/L_{\odot} = 6.7 \times 10^4 (D/2\ \mathrm{kpc})^2$, where D is the distance to AFGL 2591 in kiloparsecs. Roughly half the luminosity is observed between 2 and 20 μm, as the figure shows.

The 2-20 μm spectrum of AFGL 2591 mimics very closely the shape of a blackbody, excluding the 10 μm "silicate" feature. By fitting a Planck distribution to the observed points, we can obtain estimates of the temperature of the warm dust and the angular size of the emitting region. We find that the observed points fit very closely a blackbody distribution given by a temperature, $T_D = 460$ K, and a source diameter, $\Theta = 0.''13$. This source diameter is consistent with measured upper limits to the source sizes obtained by speckle interferometry $\Theta \leq 0.''2$ at 2.2 μm; (Howell, McCarthy, and Low 1981); $\Theta \leq 0.''5$ at 10 μm (D. Mozurkewich, private communication). However, the derived dust temperature and source size are actually lower limits to the true values since the 10 μm absorption feature suggests that the infrared source is heavily extinguished.

The far-infrared spectrum can likewise be fit fairly well by a blackbody spectrum, but this is due in a large part to the small number of filters we used. Figure 3 shows a best fit, assuming that the intrinsic spectrum is, in fact, a blackbody. The resultant values (T_D = 73 K, with Θ=8") are actually lower limits to the true values. For example, most far-infrared spectra are assumed to arise from optically-thin isothermal dust emission and that the source spectrum is of the form $F_\nu \propto \nu\ B_\nu(T)$. If this is the case for AFGL 2591, then $T_D \approx$ 110 K. However, Thronson and Harper (1984) have emphasized that overlying, non-emitting dust can alter a far-infrared spectrum and make it appear significantly "cooler" than the true dust temperature. In addition to this, Thronson and Harper further argue that for the vast majority of sources observed to date, there is not sufficient spectral coverage to determine with certainty whether or not this effect is taking place. Since this is the case for our data on AFGL 2591, we are limited to saying that the dust that dominates the far-infrared emission is characterized by $T_D \geq 73$ K, although more likely, $T_D \approx 100$ K.

The blackbody fits to the spectrum of AFGL 2591 enable us to estimate the total luminosity of the source including the contribution from emission outside the observed wavelength range. Integrating under the two black body curves, we estimate a total luminosity of 9×10^4 $(D/2\ \mathrm{kpc})^2\ L_\odot$ for the source.

Finally, the excellent pointing characteristics of the WIRO 2.3 m telescope enabled us to measure the absolute position of the N band (10 μm) emission to an accuracy of ±1" (Table 2). This represents a

substantial improvement over previous position estimates of AFGL 2591 made at 3.5 μm with ±2" accuracy (Wynn-Williams et al. 1977). The location of the 10 μm source is shown in Figure 1 relative to the locations of the H_2O maser associated with AFGL 2591 and continuum emission from compact HII regions in the vicinity (Wynn-Williams et al., Simon et al. 1981). Our improved position determination shows that the maser spot and IR source are not coincident, as previously thought. The infrared source is significantly displaced from the compact HII regions as first determined by Wynn-Williams et al. (1977). We note that our simple interpretation assumes that 3.5 μm emission arises from the same material as does the 10 μm emission.

IV. DISCUSSION

a) Nature of AFGL 2591

As shown in Figure 1 the immediate vicinity of AFGL 2591 contains two compact radio continuum sources and an H_2O maser spot, as well as the compact near-infrared source. In addition, two smaller, less bright compact continuum sources are also known to be contained within this region (Campbell 1984). The compact continuum source southwest of the infrared source has been studied by many authors (Wendker and Baars 1974, Wynn-Williams et al. 1977, Simon et al. 1981, Brown 1974, Campbell 1984) and although the fluxes determined between 2-15 GHz are not in particularly good agreement, they are consistent with a spectrum of an optically thin, photoionized HII region. If all four continuum sources are optically thin H II regions within the cloud and are photoionized by individual ZAMS stars they would contribute about 2×10^4 $L_\odot$ to the total far-infrared luminosity in the region. That is about 25% of the total luminosity we estimated for the region from our far-infrared observations. However there appears to be no strong 2 μm or 10 μm sources at any of these positions, and it is likely that these compact continuum sources are not powered by stars which contribute significantly to the far-infrared luminosity we observed. Indeed, Thompson and Tokunaga (1979) have suggested that the ionization of the H II region southwest of the infrared source is provided by UV radiation escaping from a hole in an otherwise thick dust shell around AFGL 2591. Such a model also provides a natural explanation for the presence of the

reflection nebula located approximately 20" southwest of AFGL 2591 on a line connecting the H II region and infrared source (Kleinmann and Lebofsky 1975). To provide the requisite amount of photoionization for the compact H II region, AFGL 2591 must produce an ionizing flux equivalent to that of at least an 07.5 ZAMS star. Since the luminosity of an 07.5 star is about 8×10^4 $L_\odot$ (Panagia 1974), our estimated total luminosity for AFGL 2591 of 9×10^4 $L_\odot$ is consistent with the idea that AFGL 2591 could be the source of inoization for at least the largest compact continuum source in the region. Our observations would be consistent with this model as long as the distance to AFGL 2591 is greater than 1 kpc. Clearly, our observations support the suggestion that AFGL 2591 is the dominant energy source in the region.

As the dominate energy source, AFGL 2591 would also be the driving source of the bipolar molecular flow. Since it is believed that such outflows are driven by winds emmanating very close to the surface of the central young stellar objects (e.g., Lada 1984), it is not surprising that holes or channels exist in a dust shell which would permit UV radiation to escape and ionize the compact HII region as well as produce the observed reflection nebula. Indeed, reflection nebula are found associated with many molecular outflows (Strom 1983). The existence of weaker HII regions near AFGL 2591 (see Figure 1, Simon et al. 1981 and Campbell 1984) may indicate that the dust shell is beginning to break up. However, it is also possible that the radio continuum emission is being produced by collisional ionization in a stellar wind (Krolik and Smith 1981). This certainly appears to be the case for a number of

compact HII regions associated with other high-velocity outflows (e.g., Simon et al. 1981; Cohen, Bieging and Schwartz 1982; Bally and Predmore 1983; and others). Although the existing radio spectra of AFGL 2591 are not presently suggestive of such a situation, high spectral resolution infrared recombination line observations might be able to distinguish between an outflowing collisionally ionized wind and a photo-ionized HII region. In addition sensitive searches for near-infrared sources at the site of the strongest continuum source should easily uncover a B0.5 star if one was actually ionizing the HII region. At 2.2 μm a B0.5 star at the distance of AFGL 2591 would have an apparent magnitude of +10 if extinguished by 50 visual magnitudes. However if such a star was present we should have detected it at 10 μm.

If we assume that the compact near-infrared object is the source of all the observed far-infrared emission, we can place interesting constraints on its nature. As pointed out earlier, the presence of a deep 10 μm silicate absorption feature in the spectrum indicates that between 2-20 μm we are observing heavily reddened emission from hot dust surrounding a recently formed star. An upper limit to the extinction to this hot dust can be estimated by de-reddening the near infrared observations and then requiring that the resulting total luminosity between 2-20 μm not exceed 9×10^4 $L_\odot$. If we assume a standard interstellar reddening law (e.g., Van de Hulst curve no. 15 [Johnson 1968]) we find an upper limit to the extinction of about 50 visual magnitudes between 2.3 μm and 4.9 μm. We can obtain a lower limit to the extinction from the depth of the 10 μm absorption feature.

Rieke and Lebofsky (1984) have found that $A_V = 16.6 \pm 2.1 \times \tau_{si}$ from careful measurements of a number of heavily obscured sources. Merrill and Soifer (1974) estimated an optical depth of $\tau_{si} = 1.8$ for the silicate feature in AFGL 2591. This corresponds to $A_V = 29.9 \pm 3.8$ magnitudes. This is a lower limit to the total extinction, since there is likely to be emission as well as absorption present at 10 μm. Therefore the observed depth of the silicate feature underestimates the actual extinction to the source. We conclude that AFGL 2591 is obscured by 26-50 magnitudes of visual extinction.

The presence of such a large amount of extinction towards the near-infrared emitting dust also suggests that the circumstellar dust is quite hot with tempertures in excess of 500 K. The compact nature of the near-infrared source further suggests that the range in temperature of the hot circumstellar dust may be small. For example, let us assume that the circumstellar dust has an intrinsic energy distribution of a single temperature blackbody between 2 and 5 μm. If we require the total luminosity of this blackbody to equal that of AFGL 2591, then, in principle, we can uniquely determine its temperature and size, once we specify the flux density of the blackbody distribution at any single wavelength. Because all the observed emission between 2 and 5 μm suffers considerable extinction we are uncertain of the intrinsic flux at any given wavelength. However we know that the extinction to the hot dust is between 26 and 50 visual magnitudes. Therefore if we assume an extinction law and a single value of visual extinction we can de-redden the 2-5 μm observations and attempt to fit the de-reddened points by a

blackbody whose total luminosity equals that of AFGL 2591. For possible extinctions between 26 and 50 visual magnitudes and an extinction law given by curve #15 of Van de Hulst (Johnson 1968), we find that the de-reddened observations can be fit by a single temperature blackbody of appropriate luminosity only when $A_V \gtrsim 43$ magnitudes. The resulting blackbody curve is characterized by a temperature of about 800 K and a size of about 0.06 arc seconds. Figure 3 shows the curve fit to the de-reddened observations between 2 and 5 μm.

It is of interest to compare the blackbody curve with our 8-13 μm observations. Using the extinction law derived by Rieke and Lebofsky (1984) between 8 μm and 13 μm we can predict the fluxes in this wavelength range expected from silicate absorption of the underlying blackbody emission if $A_V \gtrsim 43$ magnitudes. We find that the predicted fluxes in the silicate absorption feature are about 1.5 times smaller than that actually observed between 8.0 μm and 11.4 μm. In other words it appears that the extinction at 10 μm is equivalent to only about 23 visual magnitudes. However this may still be consistent with our single temperature dust shell model, since we expect the silicate feature to have a significant emission component. Longward of 13 μm the observed fluxes are greater than that of the blackbody curve and at these wavelengths our assumption of dust emitting at a single temperature breaks down. In any event, our observations are consistent with and perhaps best represented by a simple model for AFGL 2591 in which a single object surrounded by a hot ($T_D \gtrsim 800$ K), compact ($\theta \gtrsim .06''$) dust shell is the source for all the observed far-infrared emission.

b) The Nature of the Molecular Outflow

Our CO observations are not comprehensive enough to enable as thorough an analysis of the physical properties of this molecular outflow as has been possible for a number of other well studied sources (e.g., NGC 2071, Bally 1982; AFGL 490, Lada and Harvey 1981; AFGL 961, Lada and Gautier 1982). However, despite these limitations our observations do show AFGL 2591 to be associated with one of the more interesting of the known examples of high-velocity molecular outflow. We will now consider briefly some of the more interesting aspects of the outflow revealed by our data.

First, we find the flow to be bipolar, and as indicated by Figure 2, the spatial separation of red and blue high-velocity components is as distinct as has been found for any other flow observed to date. However, our observations are not sufficiently extensive to determine the full extent or degree of collimation of the flow. Clearly further mapping is needed to address these particular issues.

Second, we find that the velocity extent of the high-velocity gas is as great in the outermost regions of the flow as it is at the position of the infrared source at the apparent center of the bipolar flow. Thus, there is no evidence for any flow deceleration with distance from the central source. In fact, the velocity extent of the high-velocity emission is somewhat higher in the outer regions than near the center of the grid. Such kinematical behavior is not so clearly evident in any other extended source we have studied. Acceleration, or lack of deceleration, of high-velocity gas would be expected if the

force accelerating the flow was more or less constantly applied over the dynamical time scale and if the flow was propagating into a medium with a decreasing density gradient. Of particular interest in this regard is the extent of the red-shifted flow beyond the apparent boundary of the -5 km s^{-1} ambient cloud as seen in Figure 1 and discussed in Section IIA. Although, as can be seen Figure 2, there <u>is</u> weak emission ($T_A^* \gtrsim 1.4$ K) at -5 km s^{-1} in the outer red-shifted region it is not clear whether or not this emission in fact originates from ambient gas in the outermost regions of the -5 km s^{-1} cloud. The intriguing possibility remains that in these more extended regions even emission observed at -5 km s^{-1} arises in the molecular outflow rather than from ambient material. Observations of ^{13}CO emission are necessary to investigate this possibility. Even if ^{13}CO observations were to show that emission at -5 km s^{-1} arose in the quiescent part of the cloud, it is still clear from Figure 1 that the red-shifted flow component has broken out into the outermost, low density regions of the molecular cloud. It is possible that this flow component is freely expanding and that its extent is considerably larger than suggested by our map. Recently, Schwartz, Smith and Waak (1983), have suggested that the red-shifted flow associated with NGC 1333 outflow is expanding into a very low density region of that cloud. However the AFGL 2591 flow may be the first molecular outflow which appears to have expanded beyond the boundaries of its associated molecular cloud.

Third, we find the peak integrated intensity in the blue flow to be considerably greater than that in the red flow. This is similar to the situation for the S140 outflow (Lada and Wolf 1983) but not typical of

outflow sources which generally have their strongest emission in the red component (Bally and Lada 1983). Although it is not all clear what produces such asymmetries in the flow line profiles, the apparent enhancement of blue emission in AFGL 2591 could be due to the fact that the blue flow is propagating into a higher density region than the red flow, sweeping up more material in a smaller area and appearing brighter. In this case we would expect the blue flow to be considerably more confined than the red flow. Future mapping could reveal if this was the case.

Fourth, our data enables us to make crude estimates of the flow extent and dynamical age. From Figure 1 we estimate the flow to be at least 5' in extent, which corresponds to a size of 3 pc at a distance of 2 kpc. This, coupled with the observed velocity extent of the flow ($\sim$ 40 kms^{-1}), suggests a dynamical time scale of $\sim 7 \times 10^4$ years (at 2 kpc distance). These parameters indicate that the AFGL 2591 flow is one of the most extended and perhaps evolved of the known molecular outflow objects. AFGL 2591 may also be the most luminous driving source of the known molecular flow sources. It is perhaps surprising that such a luminous young stellar object has not had time enough to evolve to the point where it has produced a significant compact HII regions, yet has had enough time to generate one of the most extended outflows known. Consider that the molecular flow associated with IRc 2 in Orion (the only other well studied outflow source of comparable luminosity to AFGL 2591) has an extent of 0.2 pc and a dynamical age of $\sim 10^3$ years.

The lack of a developed HII region around AFGL 2591 might be due to the fact that the exciting star is surrounded by an extraordinarily

dense and dusty shell which has severely retarded the expansion of an HII region. However, the presence of weak continuum sources near AFGL 2591 suggests that the dust shell is breaking apart as discussed earlier.

It is also possible that AFGL 2591 is closer than 2 kpc. At a distance of 1 kpc it would have a luminosity of 2×10^4 $L_\odot$, a flow extent of $\sim$1.5 pc and flow dynamical age of 3×10^4 years, typical of the majority of luminous molecular outflow sources.

Finally, we comment on the relation of the H_2O maser to AFGL 2591 and the molecular flow. Our data indicate that AFGL 2591 is embedded in the -5 km s^{-1} cloud. Moreover it is not coincident with the H_2O maser source as previously thought. The velocity of maser emission of -21 km s^{-1} and -23 km s^{-1} (Wynn-Williams et. al 1977) clearly shows the maser source within the blue-shifted high-velocity flow. It is apparently a dense clump of gas accelerated to high-velocity by the outflow. Its close proximity to AFGL 2591 again suggests that the origin of the outflow occurs very near the infrared star.

V. SUMMARY

The primary results of our infrared and millimeter-wave study of AFGL 2591 can be summarized as follows:

1) The luminosity observed between 2 m and 160 m for the AFGL 2591 source is found to be 6.7×10^4 $(D/2\ \mathrm{kpc})^2$ $L_\odot$, suggesting a total luminosity at all wavelengths of about 9×10^4 $L_\odot$ for a source distance of 2 kpc.

2) The near- and far-infrared observations are consistent with and best explained by a model in which a single embedded object is the sole source of the observed near- and far-infrared luminosity. This object appears to be surrounded by a compact, optically thick dust shell with a temperature of $\sim$800 K and an angular diameter of $\sim$0.06", although a significant range in temperatures probably actually exists. The extinction to this source is estimated to be about 43 visual magnitudes.

3) In addition, our data are consistent with the suggestion of Thompson and Tokunaga (1979) that AFGL 2591 is the source of ionization for the compact HII regions in its vicinity and the source of scattered light for a nearby reflection nebula. As the dominant energy source in the region, AFGL 2591 is probably the sole source driving the high velocity molecular outflow associated with it.

4) Our CO observations indicate that the high-velocity molecular outflow associated with AFGL 2591 is extended and bipolar in nature.

5) The red-shifted component of the bipolar outflow appears to extend beyond the boundary of the ambient cloud in which AFGL 2591 is

embedded. The lack of significant deceleration of the red-shifted flow may be consistent with its propagation into a regime of low cloud density. The blue-shifted component of the flow is considerably brighter than the red-shifted flow in the vicinity of the infrared source, and appears to be within the cloud boundary. However, it also shows no significant deceleration with distance from the flow center. The material giving rise to both velocity components may be undergoing constant acceleration.

6) CO observations also indicate that the molecular cloud within which AFGL 2591 is embedded has an LSR velocity of -5 km s^{-1}. The velocities (i.e., -21 and -23 km s^{-1}) of the H_2O maser source associated with AFGL 2591, suggest therefore that the maser source is actually part of the blue-shifted high-velocity molecular flow.

7) The position of the near-infrared source has been determined to an accuracy of ±1" at 10 μm and we find that the infrared source is not coincident with the H_2O maser spot as previously thought. However, the close proximity of the maser spot to the infrared source does suggest that the high-velocity molecular flow originates very close to the embedded star.

We thank D. A. Harper and R. Loewenstein for providing their fine detection systems and excellent logistical support for the airborne observations. We are grateful to Dr. S. P. Willner and Dr. N. S. Woolf for helpful suggestions and discussions. We thank D. Mozurkewich for his speckle data in advance of publication. We also appreciate the continued fine support of the NASA Medium Altitude Missions Branch at Ames and the air and ground crews of the Kuiper Observatory. This work was supported by NASA Grant NAG 2-134 and NSF Grant AST 8210643. Infrared astronomy at the University of Wyoming is supported by the National Science Foundation and the United States Air Force.

W. Glaccum

Yerkes Observatory
Williams Bay, WI 53191

C. J. Lada

Steward Observatory
University of Arizona
Tucson, AZ 85721

P. R. Schwartz and H. A. Smith

E. O. Hulburt Center for
Space Research
Code 4138
Naval Research Lab
Washington, D.C. 20375

H. A. Thronson, Jr.

Dept. of Physics and Astronomy
University of Wyoming
Laramie, WY 82071

TABLE 1

PEAK AND INTEGRATED CO TEMPERATURES

Position[a]	T_A^*(K) (+1 km s^{-1} cloud)	$\int_{-21.9}^{-10.2} T_A^* dv$ (K-km s^{-1})	$\int_{3.9}^{14.5} T_A^* dv$ (K-km s^{-1})	11 m or 12 m
2E 3N	5.0	1.84	7.63	12
2E 1N	4.5	0.62	5.82	12
2E 0N	4.7	1.41	3.88	12
1E 2N	4.9	1.94	4.78	12
1E 1N	2.7	0.70	4.69	11
1E 0N	4.1	5.51	4.50	11
1E 1S	4.5	0.67	3.56	12
1E 2S	4.0	1.53	1.70	12
0 2N	5.4	$\lesssim$ 0.3	1.92	12
0 1N	4.9	17.71	7.39	11
0 ½N	5.5	25.66	5.86	11
0 0	5.4	25.85	6.39	12[b]
0 1S	4.6	9.54	2.31	12[b]
0 2S	4.6	3.74	1.44	12
½W ½N	3.4	10.71	2.73	11
1W 2N	5.9	1.26	3.51	12
1W 1N	5.5	5.09	3.62	11
1W 0N	5.2	5.00	4.42	11
1W 1S	5.0	9.53	$\lesssim$ 0.3	12[b]
1W 2S	4.7	2.27	0.47	12
2W 1S	5.2	6.29	2.11	12

[a]All positions listed in arcminute offsets from the center position: (1950) $\alpha = 20^h27^m35^s.9$ $\delta = +40°01'16"$.

[b]These positions were observed with both the 12-m and 11-m telescopes. Only the 12-m values are listed.

TABLE 2

AFGL 2591 Source Parameters

α(1950)	$20^h\ 27^m\ 35^s.8 \pm 0^s.1$
δ(1950)	$40°\ 1'\ 14" \pm 1"$

Infrared Photometry

WIRO (6".6 Aperture)[a]

2.3 μm	2.8 Jy
3.6	70
4.9	230
7.9	610
8.7	320
10.0 (N)	330
11.0	190
11.4	270
12.6	680
19.5	630
23.0	920

KAO (49" Aperture)[b]

60 μm	4600 Jy
95	5800
110	5500
160	3400

Luminosity (2-200 μm, 2 kpc) $6.7 \times 10^4\ L_\odot$

T_D (40-200 μm) = 73K; Θ = 8"

T_D (2-20 μm) = 460K (observed); Θ = 0.13"

T_D (2-20 μm) = 800K (de-reddened)[c]; Θ = 0.06"

A_V = 43 mag[c].

[a]The statistical uncertainty of the flux densities is in all cases better than 2%. The calibration uncertainty is estimated to be ±5% at 2.3 μm, 3.6 μm, and 4.9 μm. At the longer wavelengths, we estimate a ±10% calibration uncertainty.

[b]We estimate a total uncertainty of ±20%.

[c]See text.

REFERENCES

Bally, J. 1982, Ap. J., 261, 558.

Bally, J., and Lada, C. J. 1983, Ap. J., 265, 824.

Bally, J., and Predmore, R. 1983, Ap. J., 265, 778.

Becklin, E. E., Matthews, K., Neugebauer, G., and WIllner, S. P. 1978, Ap. J. 220, 831.

Brown, R. L. 1974, Ap. J. Letters, 194, L9.

Campbell, B. G. 1984, submitted to Ap. J.

Cohen, M., Bieging, J. H., and Schwartz, P. R. 1982, Ap. J., 253, 707.

Gehrz, R. D., Hackwell, J. A., and Jones, T. W. 1974, Ap. J., 191, 675.

Gillett, F. C., Jones, T. W., Merrill, K. M., and Stein, W. A. 1975, Astr. and Ap., 45, 77.

Howell, R. R., McCarthy, D. W., and Low, F. J., Ap. J. Letters, 251, L21.

Johnson, H. L. 1968, Nebulae and Interstellar Matter, ed. B. M. Middlehurst and L. H. Aller (Chicago: Univ. of Chicago Press), p. 167.

Kleinmann, S. G., and Lebofsky, M. J. 1975, Ap. J. Letters, 201, L91.

Krolik, J. H., and Smith, H. A. 1981, Ap. J., 249, 628.

Lada, C. J. 1984, in preparation.

Lada, C. J., and Gautier, T. N. 1982, Ap. J., 261, 161.

Lada, C. J., and Harvey, P. M. 1981, Ap. J., 245, 58.

Lada, C. J., and Wolf, G. 1984, in preparation.

Loewenstein, R. F. et al. 1977, Icarus, 31, 315.

Merrill, K. M., and Soifer, B. T. 1974, Ap. J. Letters, 251, L21.

Panagia, N. 1973, A.J., 78, 929.

Rieke, G., and Lebofsky, M. 1984, Ap. J. in press.

Strom, S. E. 1983, preprint.

Schwartz, P. R., Waak, J. A., and Smith, H. A., 1983, Ap. J., 267, L109.

Simon, M., Righini-Cohen, G., Felli, M., Fischer, J. 1981, Ap. J., 245, 552.

Thompson, R. I., and Tokunaga, A. T. 1979, Ap. J., 231, 736.

Thronson, H. A., and Harper, D. A. 1979, Ap. J., 230, 133.

Thronson, H.A., and Harper, D. A. 1984, Ap. J., submitted.

Thronson, H. A., and Lada, C. J. 1983, Ap. J., 269, 175.

Torrelles, J. M., Rodriguez, L. F., and Canto, J., Marcaide, J., and Ghulbudaghian, A., 1983, preprint.

Wendker, H. J. and Baars, J. W. M. 1974, Astr. Ap., 33, 157.

Willner, S. P. et al. 1982, Ap. J., 253, 174.

Wynn-Williams, C. G., 1982, Ann. Rev. Astr. Ap., 20, 597.

Wynn-Williams, C. G., Becklin, E. E., Forster, J. R., Matthews, K., Neugebauer, G., Welch, W. J., and Wright, M. C. H. 1977, Ap. J. Letters, 211, L89.

FIGURE CAPTIONS

Figure 1

Contour map of peak $T_A^*(^{12}CO)$ emission from the -5 km s^{-1} molecular cloud near AFGL 2591. Contour intervals are in steps of 2 K starting with the outermost contour which is 4 K. Also plotted are the approximate boundaries of the red- and blue-shifted components of the high-velocity molecular flow, showing the apparent bipolar nature of the flow. The positions where ^{12}CO observations were taken are indicated by "+" symbols. The location of the most intense integrated emission in the red-shifted flow is indicated by "+". The "x" symbols mark the location where the spectra shown in Figure 2 were obtained. The insert shows the small-scale structure of AFGL 2591. The 10 μm peak is presented in relation to the H_2O maser position (Wynn-Williams et al. 1977) and radio continuum emission (adapted from Simon et al. 1981).

Figure 2

The ^{12}CO spectra observed at the two locations indicated in Figure 1 by the "x" symbols. The distinct assymetry of the red and blue-shifted high-velocity line wings is clearly evident, indicative of a bipolar flow pattern. Also evident are the quiescent ambient clouds at $V_{LSR} \approx +1$ km s^{-1} and -5 km s^{-1}.

Figure 3

The observed infrared spectrum of AFGL 2591, along with simple models of the continuum emission at these wavelengths. The observed points are connected by straight lines. Our suggested models for the

mid-infrared and the far-infrared emission are the two Planck functions labeled by temperature and angular diameter. Three shorter wavelength points are shown after correction for A_V = 43 mags. The total uncertainties in each flux density measurement are shown as $\pm 1\sigma$ error bars, if they are larger than the symbol.

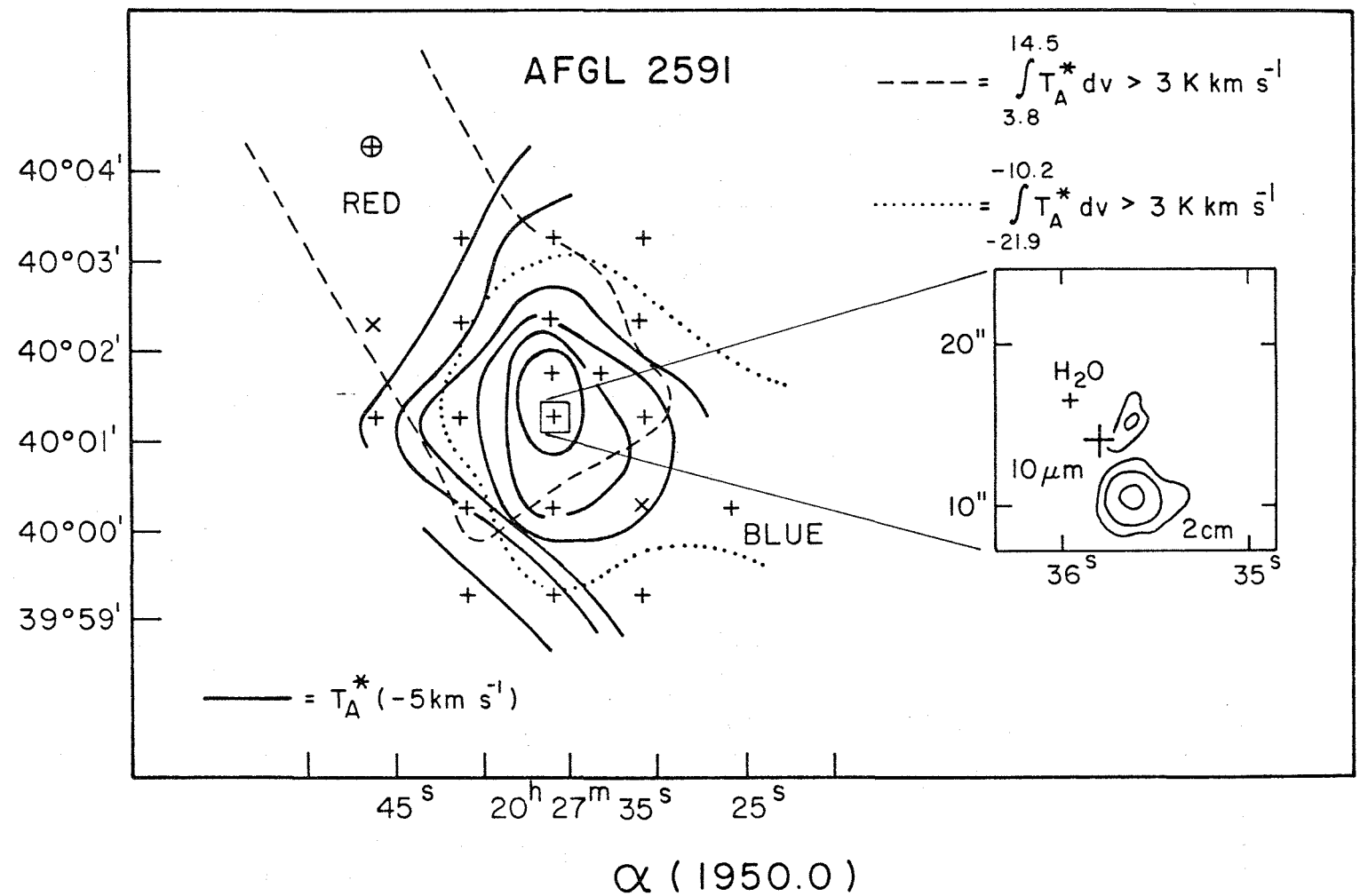
AFGL 2591
RED
BLUE
40°04'
40°03'
40°02'
40°01'
40°00'
39°59'
δ (1950.0)
45 s
20h 27m 35 s
25 s
α (1950.0)
= T_A* (-5km s-1)
= ∫ T_A* dv > 3 K km s-1 (3.8 to 14.5)
= ∫ T_A* dv > 3 K km s-1 (-21.9 to -10.2)
20"
10"
H2O
10 μm
2cm
36 s
35 s

Fig. 1

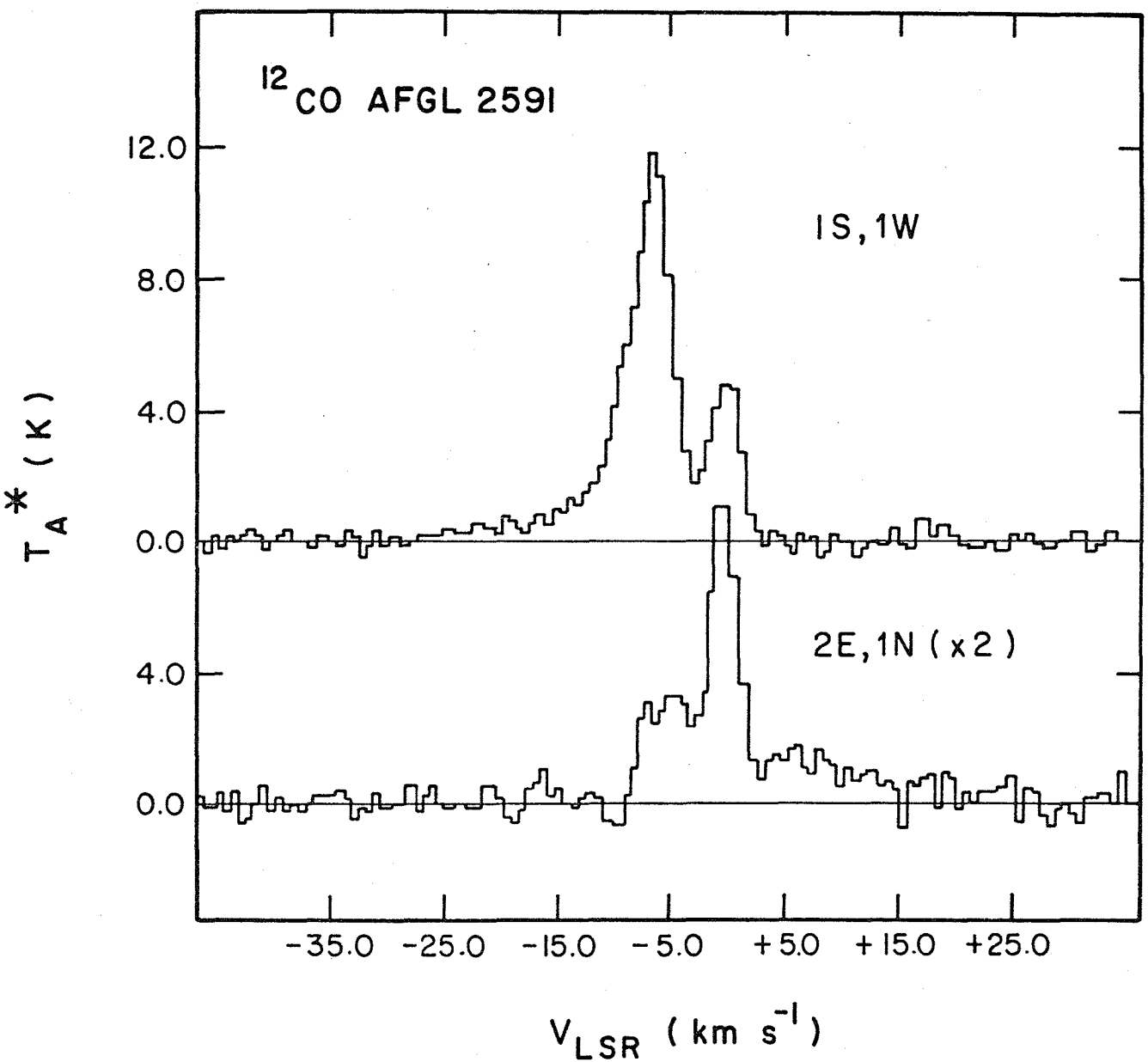
^{12}CO AFGL 2591
1S, 1W
2E, 1N (x2)
12.0
8.0
4.0
0.0
4.0
0.0
T_A^* (K)
-35.0 -25.0 -15.0 -5.0 +5.0 +15.0 +25.0
V_{LSR} (km s^{-1})

Fig. 2

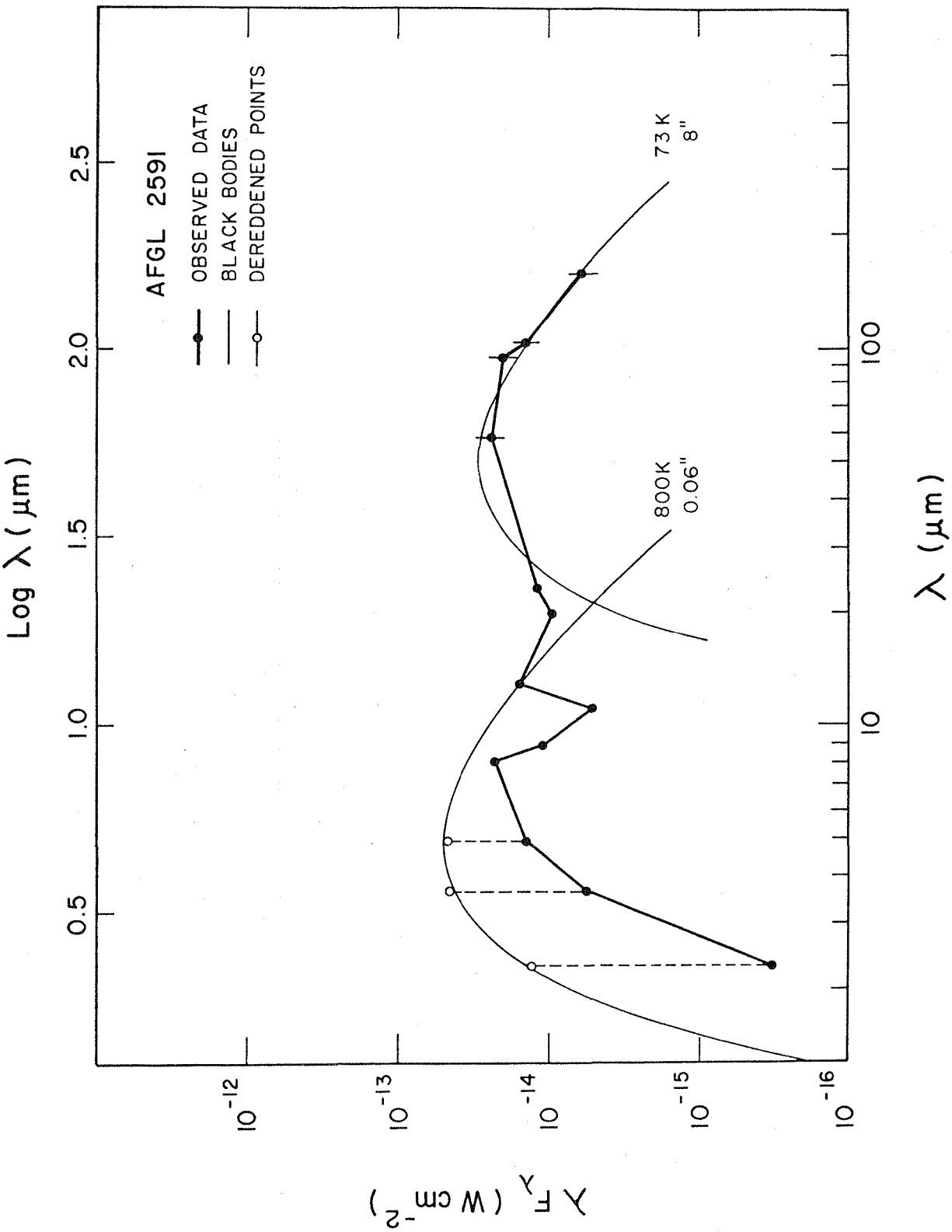
AFGL 2591
OBSERVED DATA
BLACK BODIES
DEREDDENED POINTS
73 K
8"
800K
0.06"
Log λ (μm)
λ (μm)
λ F_λ (W cm^-2)
0.5
1.0
1.5
2.0
2.5
10
100
10^-12
10^-13
10^-14
10^-15
10^-16

Fig. 3

1. Report No.	2. Government Accession No.	3. Recipient's Catalog No.
NASA TM-85963		

4. Title and Subtitle	5. Report Date
TNE NATURE OF AFGL 2591 AND ITS ASSOCIATED MOLECULAR OUTFLOW: INFRARED AND MILLIMETER-WAVE OBSERVATIONS	May 1984
	6. Performing Organization Code

7. Author(s)	8. Performing Organization Report No.
Charles J. Lada,*† Harley A. Thronson, Jr.,† Howard A. Smith,‡ P. R. Schwartz,‡ and W. Glaccum§	A-9757
	10. Work Unit No. T-5726

9. Performing Organization Name and Address	11. Contract or Grant No.
*Steward Observatory, University of Arizona, Tucson, AZ 85721 †Wyoming Infrared Observatory, University of Wyoming, Laramie, WY 82071 ‡E. O. Hulburt Center for Space Research, Naval Research Laboratory, Washington, DC 20375 §Yerkes Observatory, University of Chicago, Williams Bay, WI 53191	

12. Sponsoring Agency Name and Address	13. Type of Report and Period Covered
National Aeronautics and Space Administration Washington, DC 20546	Technical Memorandum
	14. Sponsoring Agency Code 352-02-03

15. Supplementary Notes

Preprint Series #18. Supported by NASA grants. Point of Contact: L. C. Haughney, Ames Research Center, M/S 211-12, Moffett Field, CA 94035 (415) 965-5339 or FTS 448-5339

16. Abstract

The results of infrared photometry from 2 μm–160 μm of AFGL 2591 and ^{12}CO observations of its associated molecular cloud and high velocity molecular outflow are presented and discussed. Observations between 60 μm and 160 μm provide the first detailed far-infrared spectrum of this source. The observed luminosity between 2 μm and 160 μm is 6.7×10^4 $L_\odot$ at a distance of 2 kpc. We estimate the total luminosity to be $\sim 9 \times 10^4$ $L_\odot$. The 2 μm to 160 μm spectrum of AFGL 2591 is interpreted in the context of a model in which a single embedded object is the dominant source of the infrared luminosity. We determine this object to be surrounded by a compact, optically thick dust shell with a temperature in excess of several hundred degrees kelvin. We estimate the extinction to this source to be between 26 and 50 visual magnitudes. Our data is consistent with earlier suggestions that the object which powers the near-infrared source also is responsible for ionizing the compact H II regions near AFGL 2591. We have determined the absolute position of the infrared source at 10 μm to an accuracy of ±1". This indicates for the first time that the IR source and H_2O source are not coincident.

Our ^{12}CO observations show the high-velocity molecular flow near AFGL 2591 to be extended, bipolar and roughly centered on the infrared emission. The observations suggest that the red-shifted flow component extends beyond the boundary of the ambient cloud within which AFGL 2591 is embedded. The ^{12}CO observations also show that AFGL 2591 is embedded in a molecular cloud with an LSR velocity of -5 km s^{-1}. Comparing this velocity with the velocity of H_2O maser emission (~ -22 km s^{-1}) suggests that the maser source is part of the blue-shifted high-velocity molecular outflow. Its close proximity to the infrared source suggests that the origin of the molecular outflow may be very close to (within 1") the surface of AFGL 2591.

17. Key Words (Suggested by Author(s))	18. Distribution Statement
Far-Infrared: Photometry Molecular: Cloud High Velocity: Molecular	Unlimited Subject Category - 89

19. Security Classif. (of this report)	20. Security Classif. (of this page)	21. No. of Pages	22. Price*
Unclassified	Unclassified	36	A03

*For sale by the National Technical Information Service, Springfield, Virginia 22161

End of Document